PHYSICAL REVIEW D **86,** 125003 (2012)

Enhancement of field renormalization in scalar theories via functional renormalization group

Dario Zappalà
INFN, Sezione di Catania, 64 via Santa Sofia, I-95123 Catania, Italy
(Received 11 June 2012; published 3 December 2012)

The flow equations of the functional renormalization group are applied to the $O(N)$-symmetric scalar theory, for $N = 1$ and $N = 4$, in four Euclidean dimensions, $d = 4$, to determine the effective potential and the renormalization function of the field in the broken phase. In our numerical analysis, the infrared limit, corresponding to the vanishing of the running momentum scale in the equations, is approached to obtain the physical values of the parameters by extrapolation. In the $N = 4$ theory a nonperturbatively large value of the physical renormalization of the longitudinal component of the field is observed. The dependence of the field renormalization on the UV cutoff and on the bare coupling is also investigated.

DOI: 10.1103/PhysRevD.86.125003 PACS numbers: 11.10.Gh, 11.10.Hi, 11.30.Qc

I. INTRODUCTION

An important technique in continuum field theory is the functional renormalization group [1,2], which represents a powerful method to approach both perturbative and nonperturbative phenomena; it is based on the infinitesimal integration of momentum modes from a path integral representation of the theory with the help of a Wilsonian momentum cutoff [3]. The resulting functional flow equations interpolate between the microscopic theory at short distances and the full quantum effective theory at large distances.

In the past years various realizations of the functional renormalization group were developed and, among the most renowned, there are Polchinski's and Wetterich's formulations (for reviews see Refs. [4,5]). At the same time, the derivative expansion, a powerful approximation scheme that relies on a small anomalous dimension of the field, was introduced to reduce the full flow equation to a small set of treatable partial differential equations [6,7]. More recently, a different approximation scheme was presented in Refs. [8–10], where the flow, rather than being projected on the semilocal derivative expansion of the action, is projected on the n-point 1-particle irreducible vertices, so that the momentum dependence of the correlation functions is properly taken into account.

The range of application of the functional renormalization group is wide and it is especially suitable for the study of phase transitions, due to its flexibility even in the presence of strong correlations or couplings. For instance fixed point studies of Ising-like or $O(N)$ theories, including the determination of universal critical indices, were repeatedly carried out, using different versions of the renormalization group (RG) flow equation (see for instance Ref. [11] and references therein), both to analyze the properties of the theory and to test the accuracy of the method through a comparison with other field-theoretical techniques (see e.g., Refs. [12–14]).

Some attention has also been devoted to the study of the nonperturbative features of the effective action and effective potential in the presence of spontaneous symmetry breaking. In fact is it a well known result of quantum field theory [15–17] that the effective potential defined through a Legendre transformation must be convex, a property that, in the limit of infinite volume, leads to a nonanalytic behavior with a typical degenerate flat region of the potential in correspondence of the classically forbidden region between the classical minima. The convexity of the potential can only be recovered by resorting to some nonperturbative scheme (see e.g., Refs. [18]) and it has already been studied by means of RG techniques [19–28].

In this paper we analyze in detail the spontaneously broken phase of the $O(N)$-symmetric scalar theory, for $N = 1$ and $N = 4$, in four Euclidean dimensions, $d = 4$, going beyond the local potential approximation (LPA) and including the effects of the field renormalization. Instead of deriving the flow equations for the potential V and the field renormalization Z directly from an expansion of the full flow equation for the effective action around a constant field configuration, we shall derive them starting from the approach developed in Refs. [8–10] and adopting the regulator for the infrared modes introduced in Refs. [29–32], which has the specific property of optimizing the determination of the critical exponents in the LPA. This particular choice allows us to analytically perform the integration over the momentum variable, which simplifies the structure of coupled partial differential equations (PDEs) for V and Z. The aim of the present analysis is to provide a better understanding of the details of this phenomenon which, for $N = 4$ and $d = 4$, could provide some indications on the description of the broken chiral symmetry phase for a two-flavor quark model or on the mass generation mechanism in the standard model, although in both cases the similarity has serious limitations. In fact, in the former case the $O(4)$ model is in the correct universality class to describe the universal features of the chiral phase transition, but when the system is not close to the critical line, which is the case considered here, then some properties of the fermionic model could be poorly reproduced by the scalar fields. Concerning the latter case, the coupling to gauge fields is

turned off in the $O(N)$ model and therefore the massless Golstone bosons play an important role in the infrared sector of the ordered phase and this could lead to a different behavior with respect to the usual Higgs mechanism where the Goldstone are replaced by the longitudinal degrees of freedom of the massive gauge bosons which, due to their mass, are less relevant for the infrared dynamics.

An attempt to use the two coupled flow equations for V and Z in this context was already done in Ref. [24] for the simple quantomechanical problem ($d = 0 + 1$ dimensions) and in Ref. [27] for the $N = 1$ scalar theory in $d = 4$ dimensions. In both cases the proper time version of the RG flow [33–38] (which can be regarded as an approximation to the class of exact background field flows [26,39–41]) was adopted in the exponential form, which is derived by using a sharp cutoff on the proper time variable [36,42]. In the quantomechanical case the corrections induced by the inclusion of Z turned out to be in very good agreement with the (exact) Schroedinger equation output while, for the quantum field theory, a very large Z was observed in the classically forbidden region. However, in the latter case, only partial conclusions could be drawn, because the numerical instabilities in the flow equations made rather difficult the approach to the infrared (IR) limit, where all quantum modes are integrated out and the full field renormalization is obtained. On the contrary, the approach used in this paper, based on a different approximation scheme, turns out to be numerically more stable, thus allowing us to push the RG scale low enough to get a better insight of the IR region.

The scheme of the paper is the following. In Sec. II the main details of the RG flow equations and of the approximation used are recalled; the results of the numerical analysis of the potential and the field renormalization for the single field, $N = 1$, and for the $N = 4$ theory in $d = 4$ are shown in Sec. III. The conclusions are reported in Sec. IV.

II. RG FLOW EQUATIONS

The starting point of our analysis is the partition function of the theory, defined as a functional of the source $J(x)$, and also dependent on the momentum scale k,

$$\mathcal{Z}_k[J] = \int \mathcal{D}\varphi \mathrm{e}^{-S-\Delta S_k+\int_x J\varphi}, \tag{1}$$

where the usual action S is modified by the k dependent regulator, quadratic in the field φ, $\Delta S_k[\varphi]$,

$$\Delta S_k[\varphi] = \frac{1}{2}\int_q R_k(q)\varphi(q)\varphi(-q), \tag{2}$$

with

$$\int_q \equiv \int \frac{d^d q}{(2\pi)^d} \quad \text{and} \quad \int_x \equiv \int d^d x. \tag{3}$$

In order to obtain a physically relevant flow, $R_k(q)$ must suppress the modes with $q \ll k$ while allowing to integrate those with $q \gg k$ and therefore one can choose $R_k(q)$ of order k^2 in the former region and $R_k(q) \sim 0$ in the latter. In particular at $k = 0$ the regulator must vanish so that $\mathcal{Z}_{k=0}[J]$ coincides with the standard partition function $\mathcal{Z}[J]$. In this framework the following flow equation is obtained [5] ($\partial_t \equiv k\partial_k$):

$$\partial_t \Gamma_k[\phi] = \frac{1}{2}\int_q \partial_t R_k(q)[\Gamma_k^{(2)}[q, -q; \phi] + R_k(q)]^{-1}, \tag{4}$$

where $\Gamma_k[\phi]$ is the modified effective action at scale k, defined by

$$\int_x J\phi - \Delta S_k[\phi] - \Gamma_k[\phi] = \log \mathcal{Z}_k[J], \tag{5}$$

with $\phi(x) = \delta \ln \mathcal{Z}_k[J]/\delta J(x)$ and $\Gamma_k^{(2)}[q, -q; \phi]$ is the Fourier transform of the second functional derivative of $\Gamma_k[\phi]$,

$$\Gamma_k^{(2)}[x_1, x_2; \phi] \equiv \frac{\delta^2 \Gamma_k}{\delta\phi(x_1)\delta\phi(x_2)}. \tag{6}$$

Note that the term

$$G_k(q, \phi) = [\Gamma_k^{(2)}[q, -q; \phi] + R_k(q)]^{-1} \tag{7}$$

appearing in Eq. (4) is the full propagator of the action modified by the regulator ΔS_k. Then one can take the initial condition for the flow equation (4) at the scale $k = \Lambda$ where fluctuations are frozen by ΔS_k, so that $\Gamma_{k=\Lambda}[\phi] \approx S[\phi]$ and the full effective action $\Gamma[\phi]$ of the original theory is obtained as the solution of Eq. (4) when $k \to 0$, where $R_k(q)$ vanishes and all fluctuations have been integrated out.

The most straightforward approximation scheme to treat the RG flow is to express the effective action $\Gamma_k[\phi]$ through an expansion in the derivatives of the field,

$$\Gamma_k[\phi] = \int_x \left(V_k(\phi) + \frac{1}{2} Z_k(\phi)(\partial\phi)^2 + O(\partial^4) \right), \tag{8}$$

and to project the full equation (4) onto a set of flow equations for the coefficients of the expansion $V_k(\phi), Z_k(\phi), \ldots$. This projection requires an expansion of the right hand side of Eq. (4) in powers of the field derivatives or, equivalently, in powers of the momentum.

An alternative scheme has been developed in Refs. [8–10] and, below, we shall briefly recall its essential features (in the rest of this section we will follow the notation adopted in Refs. [10]). This scheme consists in an expansion in terms of the n-point functions, $\Gamma_k^{(n)}$, i.e., the nth functional derivative of $\Gamma_k[\phi]$ with respect to the field ϕ. For instance the first two equations for $n = 0$ and $n = 2$ correspond to the two following equations, respectively for the potential V_k defined in Eq. (8) and equal, up to a volume factor, to Γ_k evaluated at a constant field

configuration ϕ, and the 2-point function computed at constant ϕ:

$$\partial_t V_k(\phi) = \frac{1}{2}\int_q \partial_t R_k(q) G_k(q,\phi), \tag{9}$$

$$\begin{aligned}\partial_t \Gamma_k^{(2)}(p,\phi) = \int_q \partial_t R_k(q) G_k(q,\phi) \\ \times \Big\{ \Gamma_k^{(3)}(p,q,-p-q,\phi) G_k(q+p,\phi) \\ \times \Gamma_k^{(3)}(-p,p+q,-q,\phi) \\ - \frac{1}{2}\Gamma_k^{(4)}(p,-p,q,-q,\phi)\Big\} G_k(q,\phi).\end{aligned} \tag{10}$$

It is easy to check from the functional structure of Eq. (4) that the flow equation of $\Gamma_k^{(n)}$ involves the s-point functions with $s \leq n+2$. Therefore an approximation or truncation is needed to obtain a closed set of PDEs. As explained in Refs. [8–10] this can be realized at any fixed n, by neglecting the internal momentum q in $\Gamma_k^{(n+1)}$ and $\Gamma_k^{(n+2)}$, so that they can be written in terms of $\Gamma_k^{(n)}$ according to the following property, valid for constant field configurations,

$$\Gamma_k^{(n+1)}(\{p_i\},0,\phi) = \partial_\phi \Gamma_k^{(n)}(\{p_i\},\phi), \tag{11}$$

where the index i runs between 1 and n. In particular, for $n=2$, $\Gamma_k^{(3)}$ and $\Gamma_k^{(4)}$ in Eq. (10) are computed at $q=0$ and expressed in terms of $\Gamma_k^{(2)}$, according to Eq. (11). Thus, a closed set of two equations for V_k and $\Gamma_k^{(2)}$ is explicitly obtained in Refs. [8–10].

Our aim is to extract the coupled flow equations of V_k and Z_k from those of V_k and $\Gamma_k^{(2)}$. This is easily obtained by performing a derivative expansion of the latter, to order $O(p^2)$. To this purpose we restrict the form of $\Gamma_k^{(2)}$ according to the ansatz in Eq. (8), i.e.,

$$\Gamma_k^{(2)}(p,\phi) = Z_k(\phi) p^2 + V_k''(\phi) + O(p^4), \tag{12}$$

where the prime indicates the derivative with respect to the field ϕ. Then, the flow equation of V_k is given in Eq. (9), while the insertion of Eq. (12) into Eq. (10) gives

$$\begin{aligned}p^2 \partial_t Z_k(\phi) + O(p^4) = J_3(p,\phi)[V_k'''(\phi) + p^2 Z_k'(p,\phi)]^2 \\ - I_3(\phi)(V_k'''(\phi))^2 \\ - \frac{1}{2} I_2(\phi) p^2 Z_k''(p,\phi) + O(p^4),\end{aligned} \tag{13}$$

where we have used the notation of [10],

$$\begin{aligned}I_n(\phi) \equiv J_n(p=0,\phi) \quad \text{and} \\ J_n(p,\phi) \equiv \int_q \partial_t R_k(q) G_k(p+q,\phi) G_k^{n-1}(q,\phi),\end{aligned} \tag{14}$$

with G_k given in Eq. (7) and $\Gamma_k^{(2)}$ in Eq. (12). Finally, to obtain the flow equation of Z_k one has to expand the integral $J_3(p,\phi)$ in powers of p^2 and systematically neglect the $O(p^4)$ terms in Eq. (13) and, as the terms proportional to p^0 in the right hand side vanish, one reads the equation for $Z_k(\phi)$ from the $O(p^2)$ terms. Then, the PDEs coming from the derivative expansion to order $O(p^2)$ of the $\Gamma_k^{(2)}$ equation derived in Refs. [8–10], contain the same approximation made on the latter, namely the neglect of the internal momentum q dependence of $\Gamma_k^{(3)}$, $\Gamma_k^{(4)}$.

The extension to the $O(N)$-symmetric scalar theory is straightforward and it is also illustrated in Ref. [10]. According to the symmetry of the theory the propagator can be written in terms of its longitudinal (L) and transverse (T) components with respect to the external field

$$G_{ab}(p^2,\phi) = G_T(p^2,\rho)\left(\delta_{ab} - \frac{\phi_a\phi_b}{2\rho}\right) + G_L(p^2,\rho)\frac{\phi_a\phi_b}{2\rho}, \tag{15}$$

where

$$\rho \equiv \frac{1}{2}\phi_a\phi_a. \tag{16}$$

If the 2-point function is parametrized as

$$\Gamma_{ab}^{(2)}(p,-p,\rho) = \Gamma_A(p,\rho)\delta_{ab} + \phi_a\phi_b\Gamma_B(p,\rho) \tag{17}$$

and Γ_A and Γ_B are expressed in the following way (here the dots indicate derivatives with respect to ρ and the script k is omitted for simplicity)

$$\begin{aligned}\Gamma_A(p,\rho) = Z_A(\rho)p^2 + \dot{V} \quad \text{and} \\ \Gamma_B(p,\rho) = Z_B(\rho)p^2 + \ddot{V},\end{aligned} \tag{18}$$

then the following relations hold

$$G_T^{-1}(p,\rho) = \Gamma_A(p,\rho) + R_k(p) = Z_T(\rho)p^2 + \dot{V} + R_k(p), \tag{19}$$

$$\begin{aligned}G_L^{-1}(p,\rho) &= \Gamma_A(p,\rho) + 2\rho\Gamma_B(p,\rho) + R_k(p) \\ &= Z_L(\rho)p^2 + \dot{V} + 2\rho\ddot{V} + R_k(p),\end{aligned} \tag{20}$$

with Z_T and Z_L defined as

$$Z_T = Z_A \quad \text{and} \quad Z_L = Z_A + 2\rho Z_B. \tag{21}$$

The flow equations for V, Z_A and Z_B are

$$\partial_t V(\rho) = \frac{1}{2}\{(N-1)I_1^{TT}(\rho) + I_1^{LL}(\rho)\}, \tag{22}$$

$$p^2\partial_t Z_A(\rho) + O(p^4) = 2\rho\{J_3^{LT}(p^2\dot{Z}_A + \ddot{V})^2 + J_3^{TL}(p^2 Z_B + \dot{V})^2 - (I_3^{LT} + I_3^{TL})\ddot{V}^2\} - \frac{1}{2}I_2^{LL}p^2(\dot{Z}_A + 2\rho\ddot{Z}_A) - \frac{1}{2}I_2^{TT}p^2((N-1)\dot{Z}_A + 2Z_B) + O(p^4), \tag{23}$$

$$p^2\partial_t Z_B(\rho) + O(p^4) = J_3^{TT}(N-1)(p^2 Z_B + \ddot{V})^2 - J_3^{LT}(p^2\dot{Z}_A + \ddot{V})^2 - J_3^{TL}(p^2 Z_B + \ddot{V})^2 + J_3^{LL}\{(p^2\dot{Z}_A + 2p^2 Z_B + 3\ddot{V})^2 + 4\rho(p^2\dot{Z}_B + \partial_\rho\ddot{V})(p^2\dot{Z}_A + 2p^2 Z_B + 3\ddot{V}) + 4\rho^2(p^2\dot{Z}_B + \partial_\rho\ddot{V})^2\} - \frac{1}{2}I_2^{TT}(N-1)p^2\dot{Z}_B - \frac{1}{2}I_2^{LL}p^2(5\dot{Z}_B + 2\rho\ddot{Z}_B) - ((N-1)I_3^{TT} - I_3^{LT} - I_3^{TL})\ddot{V}^2 - I_3^{LL}(3\ddot{V} + 2\rho\partial_\rho\ddot{V})^2 + p^2 Z_B(I_3^{LT} + I_3^{TL}) + O(p^4), \tag{24}$$

with the following definitions of the integrals ($n > 1$ and α, β stand either for L or T):

$$J_n^{\alpha\beta}(p,\rho) = \int_q \partial_t R_k(q) G_\alpha^{n-1}(q,\rho) G_\beta(p+q,\rho) \quad \text{and} \quad I_n^{\alpha\beta}(\rho) = J_n^{\alpha\beta}(p=0,\rho). \tag{25}$$

The only undefined ingredient in the above flow equations is the explicit form of the regulator. There are various functional forms of $R_k(p)$, tested in many specific problems and whose properties have been studied in detail. From a practical point of view, since we are interested in the numerical resolution of a set of PDEs, it is preferable to take a particular regulator which allows us to solve analytically the momentum integrals. The cutoff [29–32],

$$R_k(q) = (k^2 - q^2)\Theta(k^2 - q^2) \tag{26}$$

(where Θ indicates the Heaviside step function) makes the resolution of the integrals particularly simple and therefore we use this regulator in our analysis.

Regarding this choice, some comments are in order. In fact the flow equations contain the derivative of the regulator with respect to the scale k and, as discussed above, the flow of Z_k is obtained after an expansion in powers of the external momentum p which, again, introduces derivatives of the regulator. The regulator in Eq. (26) has the form $x\Theta(x)$ so that its derivative $\partial_t R_k(q)$ generates two terms: the first one, $(\partial_t x)\Theta(x)$, which produces relevant contributions and the second one $x(\partial_t\Theta(x))$ which produces a term proportional to $x\delta(x)$ that vanishes under integration over the momentum q, as long as no pathologies appear in the integrand. Therefore only the first term is to be retained in the flow equations.

Then, when deriving the PDE for Z_k from the flow of the 2-point function, an expansion in the momentum p of the integral $J_3(p,\phi)$, defined in Eq. (14), to order $O(p^2)$ is necessary and this generates new terms proportional to Θ and δ functions. Also, a derivative of delta function of the form $\partial_{p_\nu}(y\delta(y))$ (with $y = k^2 - (p+q)^2$) is generated, which, due to the particular form of the variable y, can be replaced by $\partial_{q_\nu}(y\delta(y))$ and the corresponding term can be calculated by means of an integration by parts, by recalling that the structure $y\delta(y)$ gives zero contribution even when evaluated at the boundaries of the integral over the momentum variable q. After the integration by parts, by making explicit the dependence on the distributions, one finds (below, $l_{\mu\nu}(p)$ and $h^{(i)}_{\mu\nu}(p,q)$, $i = 1, 2, 3$ generically indicate regular functions appearing in the expansion and, again, $y = k^2 - (p+q)^2$),

$$\partial_{p_\nu}\partial_{p_\mu} J_3(p,\phi) = l_{\mu\nu}(p) + \int_0^{k^2} dq^2\{h^{(1)}_{\mu\nu}(p,q)[\Theta(y) + y\delta(y)]\} + \int_0^{k^2} dq^2\{h^{(2)}_{\mu\nu}(p,q)[\Theta(y) + y\delta(y)] \times [\Theta(y) + y\delta(y)] + h^{(3)}_{\mu\nu}(p,q)\delta(y)\} \tag{27}$$

and Eq. (27), evaluated at $p = 0$, contributes to the flow equation of Z_k. The terms in Eq. (27) proportional to $\Theta(y)$ or $\Theta^2(y)$ give finite contributions while, by regarding the delta function as the limit of a sequence of normal distributions, we discarded all terms proportional to $y\delta(y)$ or $(y\delta(y))^2$ or $y\delta(y)\Theta(y)$, and calculated the last term in Eq. (27), where the argument of the delta function coincides with the upper boundary of the integral, according to $\int_0^{x_0} f(x)\delta(x - x_0) = f(x_0)/2$.

In Sec. III we study the RG flow equation of a scalar theory in the broken phase in $d = 4$, concentrating on two specific cases: the $N = 1$ and the $N = 4$ theory. We use the ansatz in Eq. (8) with the following initial condition at the ultraviolet (UV) scale $k = \Lambda$

$$\Gamma_{k=\Lambda}(\rho) = \int_x \left\{\frac{1}{2}\partial_\mu\phi_a\partial_\mu\phi_a - \frac{1}{2}\phi_a\phi_a + \lambda(\phi_a\phi_a)^2\right\}, \tag{28}$$

where $a = 1$ for $N = 1$, and runs from 1 to 4 for $N = 4$. According to Eq. (28), at $k = \Lambda$ the field renormalization is 1 (for the $N = 4$ theory $Z_L = Z_T = 1$ which, in turn means $Z_A = 1, Z_B = 0$) and the potential V_Λ only contains quadratic and quartic terms in the field, i.e., the only renormalizable terms in $d = 4$. In order to restrict ourselves to the broken phase, the bare mass, related to the

quadratic term of the potential in Eq. (28), must be negative. In particular, its explicit value is fixed at -1 so that, in the following, all dimensionful variables are automatically expressed in units of the bare mass. It must also be recalled that the phase boundary is a function of the UV cutoff Λ and of the bare coupling λ, and both parameters should not be increased too much to avoid a transition to the disordered phase.

III. FIELD RENORMALIZATION IN THE BROKEN PHASE

For practical convenience, in the following numerical analysis, instead of concentrating on the flow of $Z_k(\phi)$ and $V_k(\phi)$, we focus on $Z_k(\phi)$ and $V_k'(\phi)$, i.e., on the derivative of the potential with respect to ϕ, which means that for the $O(N)$ theory, instead of using ρ, we express all variables in terms of

$$\phi \equiv \sqrt{\phi_a \phi_a} = \sqrt{2\rho}, \tag{29}$$

and, in the following we indicate with $\bar{\phi}$ the field at the minimum of the potential in the IR limit $k = 0$,

$$V'_{k=0}(\bar{\phi}) = 0. \tag{30}$$

The Green's functions of the theory are obtained from the derivatives of the effective action evaluated at the minimum configuration $\phi = \bar{\phi}$ and therefore $\bar{\phi}$ is crucial in the determination of physical observables.

So, in $N = 1$ we solve the two coupled PDEs given by Eq. (13) and the field derivative of Eq. (9), while for the $N = 4$ theory we solve the set of three PDEs for Z_A, Z_B in Eqs. (23) and (24) and the field derivative of Eq. (22) and in all cases $d = 4$. The numerical solution of our set of PDEs is obtained with the help of the numerical algorithms group routine [43] that integrates a system of nonlinear parabolic partial differential equations in the (x, t) two-dimensional plane. The spatial discretization is performed using a Chebyshev C^o collocation method, and the method of lines is employed to reduce the problem to a system of ordinary differential equations. Typically we used Chebyshev polynomials of order 3 or 4 which already provide a stable solution. The routine contains two main parameters—the number of mesh points on the "space" axis and the local accuracy Δ in the "time" integration—that can be adjusted to control the stability of the solution. The first parameter is taken in such a way that the distance between two subsequent mesh points is $\delta x \sim 10^{-3}$, 10^{-4} while Δ typically is taken between 10^{-7} and 10^{-9}. The size of the time step is adjusted at each integration step by the routine to keep the accuracy below Δ. The number of time steps required to converge is strongly dependent on the problem considered, ranging from few hundreds up to 10^7 for the hardest cases.

The resolution of the PDEs is done with the space variable constrained between $0 < \phi < \phi_{\text{bound}}$ and for our purposes $\phi_{\text{bound}} = 4$ was sufficiently large to ensure the stability of the solution. The required initial conditions for the PDEs at initial time $k = \Lambda$ and $0 < \phi < \phi_{\text{bound}}$ are implicitly given in Eq. (28). The boundaries at $\phi = 0$ in the entire range of time integration reflect the required symmetry of our model: $V_k'(0) = Z_k'(0) = 0$ while at $\phi = \phi_{\text{bound}}$ we keep free boundaries. Finally, the time integration that starts at $k = \Lambda$ should, in principle, reach $k = 0$ or at least should be pushed close enough to zero that the solution has become invariant. But in the following analysis, due to the not smooth behavior of the solution, which gets worse when approaching the point $k = 0$, the numerical integration breaks down well before $k = 0$. Clearly this is peculiar of the broken phase because in the symmetric phase, where both solution for V_k and Z_k are much smoother, one can easily reach values of the scale k where the solutions are already stable. In the broken phase the lowest accessible value of k depends on the bare parameters (larger values of Λ and λ in this sense are preferable) and also on the accuracy Δ in the time integration and on δx in the "spatial" mesh. However the process of improving space and time accuracy has the effect of increasing the computer time and in any case the routine seems to be unable to converge for k below some particular value. So the best compromise found for the minimal value of k in the present analysis is $k = 0.02$ at which the routine converges for all the examples considered.

As a first step, we set the boundary values $\Lambda = 10$ and $\lambda = 0.1$ in Eq. (28) and analyze the derivative of the potential as obtained from the two coupled PDEs for $N = 1$ (and $d = 4$). The results for $V_k'(\phi)$ are shown in Fig. 1. Curve (a) is V'_Λ, while (b), (c), (d), (e) respectively correspond to V_k' at $k = 0.7, 0.5, 0.3, 0.02$.

Together with these RG outputs we also display in Fig. 1 the derivative of the one-loop effective potential, (f), obtained with the same set of renormalized parameters of

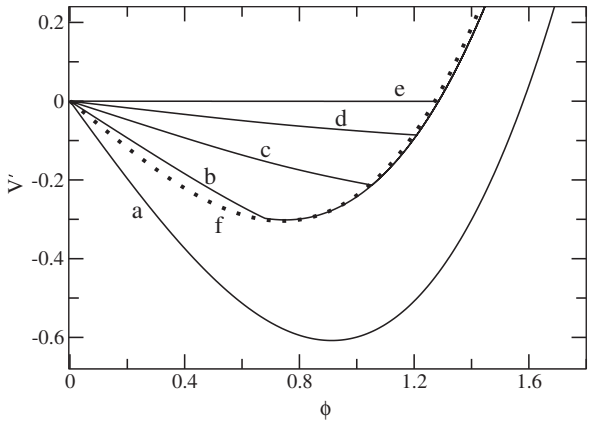

FIG. 1. $V_k'(\phi)$ for $N = 1$ and $d = 4$ at various k: $k = \Lambda$ (a), 0.7 (b), 0.5 (c), 0.3 (d), 0.02 (e), with $\Lambda = 10$ and $\lambda = 0.1$. The dotted curve (f) is the one loop effective potential derivative, $V'_{1l}(\phi)$, in terms of renormalized parameters.

curve (e). More specifically, the one loop quantum correction to the effective potential, properly regularized by a four-momentum cutoff Λ, reads (see e.g., Ref. [44])

$$V_{1l}(\phi) = \frac{1}{64\pi^2}\left\{\Lambda^4 \ln\left(1 + \frac{V_o''(\phi)}{\Lambda^2}\right) - (V_o''(\phi))^2 \ln\left(1 + \frac{\Lambda^2}{V_o''(\phi)}\right) + \Lambda^2 V_o''(\phi)\right\}, \quad (31)$$

where the prime, again, denotes the derivative with respect to the field and V_o is the bare potential which, in our case, is given in Eq. (28). In the presence of a negative square mass term and therefore of unstable modes, the logarithms in Eq. (31) develop an imaginary part and here we shall only consider the real part of the one loop effective potential.

We observe that the flow equation has a different dependence on the the ultraviolet cutoff Λ with respect to Eq. (31). This can be directly checked by integrating Eq. (9) in the LPA (i.e., fixing $Z_k = 1$) and also neglecting the k dependence of V_k in the right hand side of the equation, in order to preserve at least the leading dependence on Λ. In this case the flow equation reads:

$$\partial_k V_k(\phi) = \frac{k^5}{32\pi^2} \frac{1}{k^2 + V_o''(\phi)}, \quad (32)$$

and its integration from $k = \Lambda$ down to $k = 0$ gives the following expression of the correction to the first derivative of the bare potential:

$$V'_{\rm corr}(\phi) = \frac{V_o'''}{64\pi^2}\left\{\Lambda^2 - 2V_o'' \ln\left(1 + \frac{\Lambda^2}{V_o''(\phi)}\right) + \frac{\Lambda^2 V_o''(\phi)}{\Lambda^2 + V_o''(\phi)}\right\} \quad (33)$$

to be compared with the derivative of Eq (31),

$$V'_{1l}(\phi) = \frac{V_o'''}{64\pi^2}\left\{2\Lambda^2 - 2V_o'' \ln\left(1 + \frac{\Lambda^2}{V_o''(\phi)}\right)\right\}. \quad (34)$$

While the logarithmic term in Eqs. (33) and (34) is the same, the leading term proportional to Λ^2 has different coefficients. Equation (33) also shows an additional subleading term. However, the difference between Eqs. (33) and (34) plays no role for the renormalized quantities because it can be totally compensated by a suitable choice of the counterterms so that the absence of divergences (i.e., the cancellation of any dependence on the cutoff Λ) ensures the smallness of the one loop corrections to the classical potential. In practice this is realized by fixing the proper mass and coupling counterterms in the one loop effective potential, so that its second and fourth derivatives computed at the minimum of the one loop potential, $\bar{\phi}_{1l}$, respectively coincide with the numerical values of the (right limit) of the second and fourth derivative of the RG generated potential at $\bar{\phi}$, as obtained from curve (e). As it is evident from Fig. 1, curve (f) obtained by the above renormalization procedure is extremely close to curve (e) in the region above the minimum, with the small differences mainly referable to higher loop corrections and to $1/\Lambda^2$ terms that are neglected in our computation of the renormalized one loop potential. Instead, as is well known, the large difference between (e) and (f) in the region below the minimum is due to the failure of the perturbative expansion in recovering the convexity property of the effective potential which corresponds to the flat region of curve (e).

Before proceeding we also quote the perturbative correction of the field renormalization as obtained from a one loop calculation in [16],

$$Z_{1l}(\phi) = \frac{\lambda}{4\pi^2}\left\{\frac{V_o''(\phi) - V_o''(0)}{V_o''(\phi)}\right\}, \quad (35)$$

which has to be added to the leading term $Z_o = 1$. Equation (35), when computed at the physical value of the field, i.e., at the minimum of the potential $\bar{\phi}$, vanishes in the disordered symmetric phase ($\bar{\phi} = 0$), but it has a finite value in the broken phase, proportional to the coupling λ. In particular, in our example with $\lambda = 0.1$, the one loop correction is $Z_{1l}(\bar{\phi}) = 1.69 \times 10^{-3}$.

Let us come back to the RG generated potential. In the region of small ϕ the curves b, c, d, e show the flattening which had been already observed many times [21,23–28]: the evolution of the potential is smooth until k reaches the infrared threshold where $k^2 \simeq -V_k''(\phi = 0) > 0$, i.e., the region of the unstable modes which induce strong modifications to the propagator and therefore to the flow. When k becomes smaller than this threshold, $V_k'(\phi)$ starts to develop a linear behavior in ϕ close to $\phi = 0$ (see curve b) and, when k gets smaller, the linear region extends to larger values of ϕ with a slope that decreases toward zero. On the other hand, the region with $\phi > \bar{\phi}$ is substantially k independent for k below threshold, with only very small changes when $k \sim 0$ [see curves (c), (d), (e)]. The region between the two regimes at small and large ϕ shows a sudden change of slope that becomes sharper and sharper for lower values of k. However when the details of this sudden change are properly enlarged, the field derivatives of curves (b), (c), (d) still show a continuous behavior while for the derivative of curve (e), obtained for $k = 0.02$, the change is so sharp that, according to the numerical precision imposed, the routine is not able to approach zero beyond $k = 0.02$.

This is essentially what was expected. Indeed, it is known that at $k = 0$ the potential must reproduce the features of the effective potential which is convex, with a flat region for $-\bar{\phi} \le \phi \le \bar{\phi}$ and with a nonanalytic behavior, that consists in a jump of the second derivative of the potential at $\bar{\phi}$ from zero to a finite value. As a consequence, the computation of the zero momentum Green's functions from the derivatives of the effective potential is typically obtained by taking the limit of the

derivatives from above, $\phi \to \bar{\phi}$ with $\phi > \bar{\phi}$, while the limit from below (with $\phi < \bar{\phi}$) is associated to tunneling processes with infinitely large time scales. In our numerical analysis the "flat" part of curve (e) obtained at $k = 0.02$, is practically vanishing: it differs from zero for less than 10^{-3}. Moreover, the fact that the positive branches of (c), (d), (e) are practically coincident, implies that these curves provide a reasonably good estimate of $\bar{\phi}$ even if the flow has not reached the point $k = 0$.

We are also able to check $V_k(\phi)$ for small ϕ and k. In fact, in this regime the relation $V_k'(\phi) = -k^2\phi$ has been repeatedly derived starting from the functional form of the flow equations in the LPA (see e.g., Refs. [19,20,22,25,28]). In the example displayed in Fig. 1, the effect of Z_k is included and we have no analytical solution for the coupled PDEs; however for the curves (b), (c), (d) and (e) we find $-V_k'(\phi)/(k^2\phi) = 0.955(10)$ at $\phi = 0.1$ and $-V_k'(\phi)/(k^2\phi) = 0.930(10)$ at $\phi = 0.5$ and this gives an estimate of the size of the corrections to the above relation, which stay below 10% even for values of k and ϕ close to $\bar{\phi}/2$.

In the $N = 4$ case the derivative of the potential shows a linear behavior in the range of small ϕ and k similarly to the case $N = 1$ in Fig. 1. However for continuous symmetries in the ordered phase the presence of the Goldstone bosons has a strong impact on the infrared sector of the theory. In particular, according to the study of the susceptibility of the $O(N)$-symmetric theories ($N > 1$) [12,45,46], in $d = 4$ one expects a vanishing second derivative of the potential at $\phi = \bar{\phi}$. This means that the nonanalyticity developed in the $N = 1$ potential at $k = 0$, discussed before, should disappear in $N = 4$. To analyze this point, we plot in Fig. 2 an enlarged detail of V_k' around $\bar{\phi}$, with $N = 4$, $d = 4$, for $k = 0.02$ and $k = 0.01$. This computation is performed in the LPA at $\lambda = 0.13$ and $\Lambda = 10$, in order to get closer to $k = 0$ and have a more accurate check on the behavior of V_k'. In fact, in Fig. 2 the magnification is so large that the various mesh points can be identified but, both at $k = 0.02$ and 0.01, V_k' shows a smooth growth without apparent jumps or rapid numerical fluctuations which were instead observed in the $N = 1$ case. According to the numerical precision considered we can state that the LPA solution is approaching $V_{k=0}''(\bar{\phi}) = 0$. The inclusion of the field renormalization makes more difficult the approach to $k = 0$ but there is no qualitative modification of the picture observed in the LPA up to $k = 0.02$.

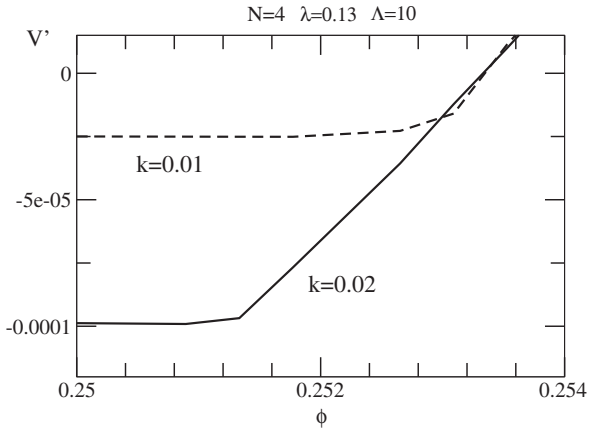

FIG. 2. V_k' for $N = 4$ and $d = 4$ at $k = 0.02$ and $k = 0.01$ in LPA with $\lambda = 0.13$, $\Lambda = 10$.

Let us now focus on the other variables, that is the field renormalization Z_k and Z_L, Z_T. The qualitative behavior of the field renormalization is already illustrated in Ref. [27]. It is essentially perturbative when k is larger than the mentioned threshold, with deviations of order 10^{-3} from 1 [see Eq. (35)]. Then, when k decreases, a bump appears for values of ϕ around the separation point of the two regimes of V_k'. When k approaches zero this bump grows, dropping very rapidly to the standard perturbative value at the separation point. In Fig. 3 the field renormalization in $N = 1$ and $N = 4$ (and $d = 4$) are shown. In the left panel of Fig. 3 we collected $Z_k(\phi)$ for $N = 1$, at $k = 0.5$ and $k = 0.02$ together with Z_T for $N = 4$, at $k = 0.3$ and $k = 0.02$. In the right panel Z_L for $N = 4$ is plotted at $k = 0.3$ and $k = 0.02$ with a much larger scale on the y axis because of the very high peak of Z_L.

Before going on, it must be remarked that the peak of $Z_k(\bar{\phi})$ for $N = 1$ in Fig. 3 is much smaller than that observed in Ref. [27] (whose value was around 10), where the proper time RG flow with sharp cutoff on the proper time variable was used. That particular version of flow equation, due to its exponential nature, although very rapidly converging and very accurate in computing the critical exponents of the Ising universality class, was criticized in Ref. [25] for not well reproducing the details of the singularity in the second derivative of the potential in

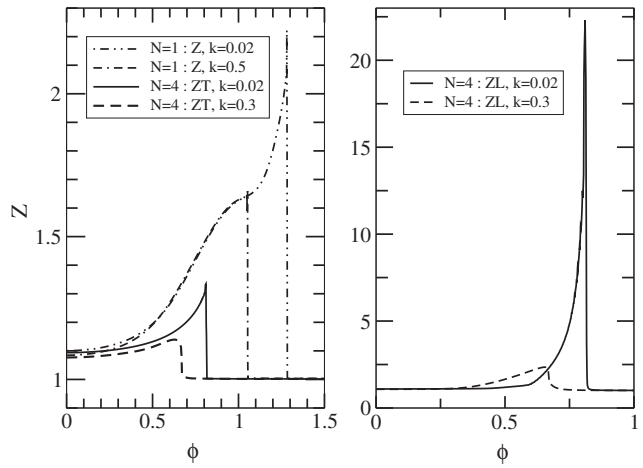

FIG. 3. Left panel: Z_k for $N = 1$ at $k = 0.5, 0.02$ (dot-dashed); Z_T for $N = 4$ at $k = 0.3$ (dashed) and $k = 0.02$ (continuous). Right panel: Z_L for $N = 4$ at $k = 0.3$ (dashed) and $k = 0.02$, (continuous). $d = 4$, $\Lambda = 10$ and $\lambda = 0.1$ for all curves.

the broken phase. According to this criticism, the large size of the peak found in Ref. [27] could be addressed to that version of the flow equation which artificially amplifies the behavior of Z_k close to $\bar{\phi}$. On the other hand the approach followed in this paper is expected to be more accurate at the quantitative level and therefore more suitable to describe this particular feature.

Going back to the curves of the field renormalization, beside the size of the peaks other differences are illustrated in Fig. 4, where an enlargement of the lowest part of Fig. 3 (only those curves at $k = 0.02$ are plotted) is shown. We note that both Z_k of the $N = 1$ theory and the transverse component Z_T of the $N = 4$ theory show a very sharp drop followed by a drastic change of slope. However, by comparing the scale of the x axis in the left and right panel of Fig. 4, it is evident that Z_k with $N = 1$ is much steeper than Z_T with $N = 4$ and, in particular, the drop observed in the $N = 1$ case is very close (within the numerical accuracy employed) to a discontinuous jump. Instead, the longitudinal component Z_L of the $N = 4$ theory smoothly approaches the perturbative regime for $\phi \sim \bar{\phi}$ and this, as shown below, yields a large (if compared with the perturbative correction), finite prediction of $Z_L(\bar{\phi})$.

The structure of the flow equation of the field derivative is more complicated than the equation of the potential and even an approximate analytic solution is missing. However, from our numerical investigation we are now able to get some hints on the dependence of Z on various parameters such as the running scale k or the bare coupling λ or the UV cutoff Λ. We concentrate on those values of ϕ where Z can be reasonably extracted, and therefore we shall examine the origin $\phi = 0$ and the point $\bar{\phi}$. We avoid instead to analyze the peak of Z which is often affected by large fluctuations.

We start by observing that in our computation in Fig. 4, for $N = 1$ the minimum is at $\bar{\phi} = 1.285$ and one finds $Z_k \sim 1.003$ for $\phi > 1.284$ at $k = 0.02$, so that a typical perturbative value is observed at $\bar{\phi}$. Then one should conclude that $Z_{k=0}(\bar{\phi}) \sim 1.003$, unless at $k = 0$ the sharp drop of Z_k hits $\bar{\phi}$, in which case no precise determination of $Z_k(\bar{\phi})$ would be possible within our numerical accuracy. The data collected when k approaches zero do not exclude either of these two alternatives. In the case of the $N = 4$ theory one has $\bar{\phi} = 0.819$ and $Z_T \sim 1.003$ for $\phi > 0.816$ at $k = 0.02$ similar to what happens in the $N = 1$ case with the difference that for $N = 1$ the jump could reasonably turn into a discontinuity, as already noticed, while in $N = 4$ the less steep drop reported in the left panel of Fig. 4 together with the smooth behavior of the potential around $\bar{\phi}$ observed in Fig. 2, suggest that Z_T could not develop a discontinuous gap at $k = 0$. On the other hand, as it is evident from the left panel of Fig. 4, the renormalization of the longitudinal field is more regular and the large peak decreases so smoothly that at $\bar{\phi}$ one finds $Z_L = 1.324$ at $k = 0.02$. Then, in this case it is possible to study the evolution of $Z_L(\bar{\phi})$ as a function of k and eventually extrapolate its value at $k = 0$.

In Fig. 5 we show some values of $Z_k(\phi = 0)$, $Z_L(\phi = 0) = Z_T(\phi = 0)$, and of $Z_L(\bar{\phi})$, obtained at small values of k. In all cases $\lambda = 0.1$, $\Lambda = 10$ and $d = 4$. For the points at $\phi = 0$ we found that the functional form

$$f(k) = ak^2 + b \tag{36}$$

provides excellent fits to the data with $a = -0.079$, $b = 1.101$ for $N = 1$ and $a = -0.216$, $b = 1.094$ for $N = 4$ and the corresponding plots are also shown in Fig. 5. As in the case of the potential, we observe here a quadratic dependence on the running scale k.

Let us now consider $Z_L(\bar{\phi})$. In this case the two expressions

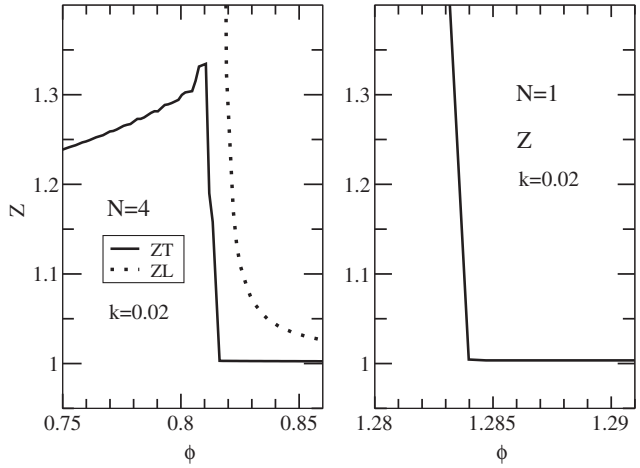

FIG. 4. Enlarged details of Fig. 3. Left panel: Z_T (continuous) and Z_L (dotted) for $N = 4$ at $k = 0.02$. Right panel: Z_k (continuous) for $N = 1$ at $k = 0.02$. $d = 4$, $\Lambda = 10$ and $\lambda = 0.1$ for all curves.

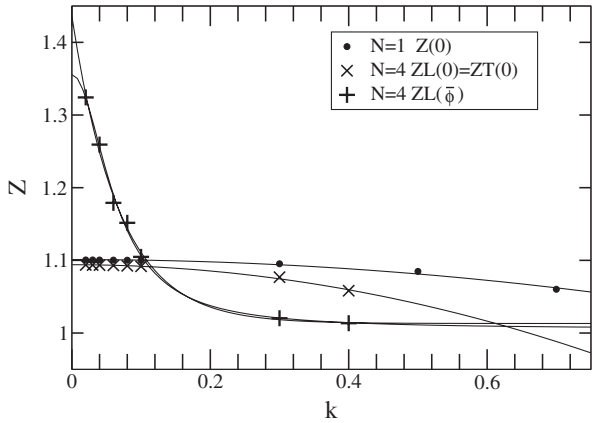

FIG. 5. $Z_k(\phi = 0)$ for $N = 1$ (black circles) and $Z_L(\phi = 0) = Z_T(\phi = 0)$ for $N = 4$ (crosses) and $Z_L(\bar{\phi})$ for $N = 4$ (plus) at various values of k. In all cases $d = 4$, $\Lambda = 10$ and $\lambda = 0.1$. Fits to these data are also plotted (see text).

$$Z_L = 1.0056 + \frac{0.0014}{k^2 + 0.0040} \quad \text{and}$$
$$Z_L = 1.0131 + 0.4225 e^{-14.6466k} \tag{37}$$

fit equally well with the data and we report both curves in Fig. 5. Their extrapolation at $k = 0$ yield two different (of about 7%) values of Z_L. However, remarkably, the fitted points do not suggest a divergent behavior of $Z_L(\bar{\phi})$ at $k = 0$, but, on the contrary, indicate finite values not very distant from that found at $k = 0.02$. We take this as a general indication that for this variable no strong modifications should be expected in the range $0 < k < 0.02$.

In Fig. 6 we show $Z_k(\phi = 0)$ and $Z_L(\phi = 0) = Z_T(\phi = 0)$ versus $y = 100\lambda$, at $k = 0.02$ and $\Lambda = 10$; we also show $Z_k(\phi = 0)$ and $Z_L(\phi = 0) = Z_T(\phi = 0)$ versus $y = \Lambda$ at $k = 0.02$ and $\lambda = 0.1$. Except for the black circles, the other points show a rapid bend downward for large y and this is due to the approaching of the critical value of λ or Λ, which signals the transition to the symmetric phase. Apart from these points the two curves associated to circles and squares have the form $g(\lambda) = a\lambda^2 + b\lambda + c$ which is a typical expansion in powers of the coupling (for completeness we find $a = -1.4823$, $b = 0.3855$, $c = 1.0700$ for the squares and $a = -1.4245$, $b = 0.5214$, $c = 1.0626$ for the circles), while the points related to the field renormalization dependence on Λ display a linear behavior in a large range of the UV cutoff.

Finally in Fig. 7 we show two plots of $Z_L(\bar{\phi})$, one versus $y = \Lambda$ with $\lambda = 0.1$ and the other versus $y = 100\lambda$ with $\Lambda = 10$. All points are collected at $k = 0.02$. We observe a small dependence on the coupling with a small increase around $\lambda = 0.1$ followed by a drop when approaching the critical line. Instead, we find a much stronger dependence on the cutoff with the field renormalization that reaches 3.5 for $\Lambda = 3$. By excluding the two points at large Λ, which

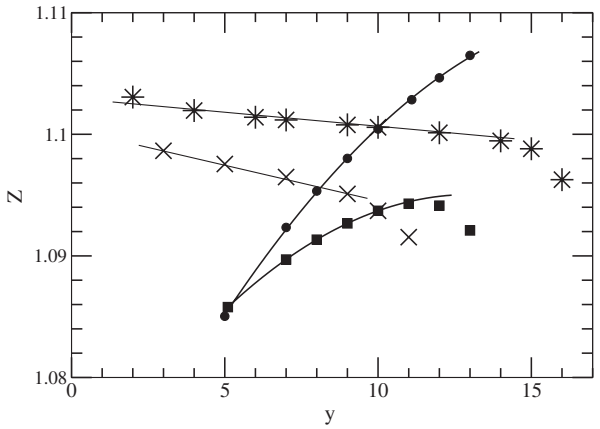

FIG. 6. $Z_k(\phi = 0)$ for $N = 1$ (black circles) and $Z_L(\phi = 0) = Z_T(\phi = 0)$ for $N = 4$ (black squares) versus $y = 100\lambda$ at $k = 0.02$ and $\Lambda = 10$. $Z_k(\phi = 0)$ for $N = 1$ (stars) and $Z_L(\phi = 0) = Z_T(\phi = 0)$ for $N = 4$ (crosses) versus $y = \Lambda$ at $k = 0.02$ and $\lambda = 0.1$. All curves are for $d = 4$. Fits to these data are also plotted (see text).

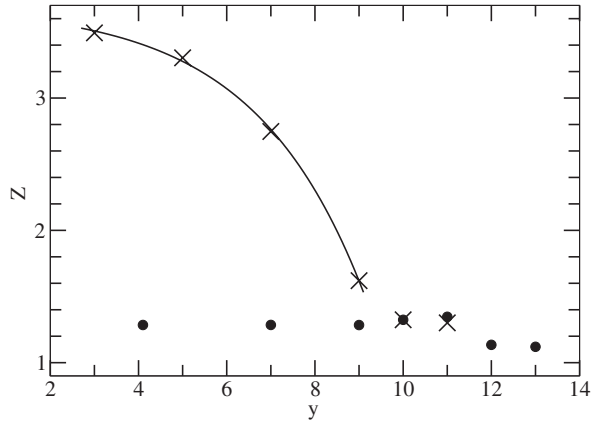

FIG. 7. $Z_L(\bar{\phi})$ for for $N = 4$ (black circles) versus $y = 100\lambda$ at $k = 0.02$ and $\Lambda = 10$. $Z_L(\bar{\phi})$ for $N = 4$ (crosses) versus $y = \Lambda$ at $k = 0.02$ and $\lambda = 0.1$. In all cases $d = 4$. A fit to the latter set of data is also plotted (see text).

are closer to the critical line, the other points are in good agreement with the curve $Z_L = 3.694 - 0.0562\, e^{0.401\Lambda}$, which can obviously be expanded in a polynomial.

IV. CONCLUSIONS

In this paper, we used the functional renormalization group to analyze the renormalization function of the scalar field in the $N = 1$ theory and of the longitudinal and transverse components in the $O(4)$-symmetric theory in four Euclidean dimensions in the ordered phase where, due to spontaneous symmetry breaking, a nonvanishing vacuum expectation value $\bar{\phi} \neq 0$ is generated. In particular, the approximation scheme of Refs. [8–10] on the RG flow equations with the cutoff in Eq. (26) provides a set of numerically stable coupled PDEs for V and Z, which allow us to approach the physical limit $k = 0$ and to determine the main features of the field renormalization.

We found that a large nonperturbative enhancement of Z occurs in the range of ϕ corresponding to the observed flattening of the potential. This effect in Z had already been observed in quantum mechanics [24] and its large value in the classically forbidden region has also a direct interpretation in terms of suppression factor of the tunneling probability of a wave packet between two vacua [17,47]. However, in field theory the numerical resolution of the equation is more problematical and a first indication of a large field renormalization for the $N = 1$ case was obtained in Ref. [27]. Our analysis qualitatively confirms those findings, but the maximum value of the peak found here is largely reduced with respect to Ref. [27].

In particular we found that for $N = 1$ the potential V_k develops a nonanalytic behavior at $\bar{\phi}$ in the limit $k \to 0$ and Z_k presents a peak followed by a sharp drop that occurs definitely for $\phi < \bar{\phi}$ at $k = 0.02$ (which is the typical lower limit reachable by our numerical routine). If this should persist even at $k = 0$, then $Z_k(\bar{\phi})$ would be substantially

perturbative; otherwise if at $k = 0$ the drop should occur at $\bar{\phi}$, then we were not able to obtain a reasonable determination of $Z_k(\bar{\phi})$. The data collected close to $k \sim 0$ do not exclude either of these two alternatives.

In the $N = 4$ theory the numerical analysis indicates that the potential does not develop a discontinuity in its second derivative with respect to ϕ, as in the $N = 1$ case, and even the transverse component Z_T shows a less sharp plot than Z_k for $N = 1$, suggesting in this case a continuous behavior at $\bar{\phi}$ and $k \sim 0$. At the same time the longitudinal component Z_L has a very high peak but the curve is so well behaved that it is possible to extract $Z_L(\bar{\phi})$ at various k and its extrapolation down to $k = 0$ remarkably leads to finite values.

The dependence of Z on the UV cutoff and on the bare coupling has also been investigated and this provides an indication on the typical numerical range spanned by the field renormalization, although it must be recalled that, quantitatively, these results are affected by large uncertainties because even a very small numerical error in the estimate of $\bar{\phi}$ induce large modifications in the determination of Z_L.

[1] J. Polchinski, Nucl. Phys. **B231**, 269 (1984).
[2] C. Wetterich, Phys. Lett. B **301**, 90 (1993).
[3] K. G. Wilson and J. B. Kogut, Phys. Rep. **12**, 75 (1974).
[4] C. Bagnuls and C. Bervillier, Phys. Rep. **348**, 91 (2001).
[5] J. Berges, N. Tetradis, and C. Wetterich, Phys. Rep. **363**, 223 (2002).
[6] T. R. Morris, Phys. Lett. B **329**, 241 (1994).
[7] D. F. Litim, J. High Energy Phys. 11 (2001) 059.
[8] J.-P. Blaizot, R. Mendez Galain, and N. Wschebor, Phys. Lett. B **632**, 571 (2006); Phys. Rev. E **74**, 051116 (2006); **74**, 051117 (2006).
[9] F. Benitez, J. P. Blaizot, H. Chate, B. Delamotte, R. Mendez-Galain, and N. Wschebor, Phys. Rev. E **80**, 030103 (2009).
[10] F. Benitez, J. P. Blaizot, H. Chate, B. Delamotte, R. Mendez-Galain, and N. Wschebor, Phys. Rev. E **85**, 026707 (2012).
[11] D. F. Litim and D. Zappalà, Phys. Rev. D **83**, 085009 (2011).
[12] J. Zinn-Justin, *Quantum Field Theory and Critical Phenomena* (Clarendon Press, Oxford, 1996).
[13] A. Pelissetto and E. Vicari, Nucl. Phys. **B522**, 605 (1998); **B540**, 639 (1999); Phys. Rep. **368**, 549 (2002).
[14] F. Parisen Toldin, A. Pelissetto, and E. Vicari, J. High Energy Phys. 07 (2003) 029.
[15] K. Symanzik, Commun. Math. Phys. **16**, 48 (1970).
[16] J. Iliopoulos, C. Itzykson, and A. Martin, Rev. Mod. Phys. **47**, 165 (1975).
[17] T. L. Curtright and C. B. Thorn, J. Math. Phys. (N.Y.) **25**, 541 (1984).
[18] Y. Fujimoto, L. O'Raifeartaigh, and G. Parravicini, Nucl. Phys. **B212**, 268 (1983); C. M. Bender and F. Cooper, Nucl. Phys. **B224**, 403 (1983); D. J. E. Callaway, Phys. Rev. D **27**, 2974 (1983); V. Branchina, P. Castorina, and D. Zappalà, Phys. Rev. D **41**, 1948 (1990).
[19] A. Ringwald and C. Wetterich, Nucl. Phys. **B334**, 506 (1990).
[20] N. Tetradis and C. Wetterich, Nucl. Phys. **B383**, 197 (1992).
[21] K.-I. Aoki, A. Horikoshi, M. Taniguchi, and H. Terao, in *Proceedings of the Workshop "The Exact Renormalization Group", Faro, Portugal, Sept. 1998* (World Scientific, Singapore, 1999), p. 194.
[22] J. Alexandre, V. Branchina, and J. Polonyi, Phys. Lett. B **445**, 351 (1999).
[23] A. S. Kapoyannis and N. Tetradis, Phys. Lett. A **276**, 225 (2000).
[24] D. Zappalà, Phys. Lett. A **290**, 35 (2001).
[25] A. Bonanno and G. Lacagnina, Nucl. Phys. **B693**, 36 (2004).
[26] D. F. Litim, J. M. Pawlowski, and L. Vergara, arXiv:hep-th/0602140.
[27] M. Consoli and D. Zappalà, Phys. Lett. B **641**, 368 (2006).
[28] J.-M. Caillol, Nucl. Phys. **B855**, 854 (2012).
[29] D. F. Litim, Phys. Lett. B **486**, 92 (2000).
[30] D. F. Litim, Phys. Rev. D **64**, 105007 (2001).
[31] D. F. Litim, Int. J. Mod. Phys. A **16**, 2081 (2001).
[32] J. M. Pawlowski, Ann. Phys. (Amsterdam) **322**, 2831 (2007).
[33] S. B. Liao, Phys. Rev. D **53**, 2020 (1996).
[34] O. Bohr, B. J. Schaefer, and J. Wambach, Int. J. Mod. Phys. A **16**, 3823 (2001).
[35] A. Bonanno and D. Zappalà, Phys. Lett. B **504**, 181 (2001).
[36] D. F. Litim and J. M. Pawlowski, Phys. Lett. B **516**, 197 (2001).
[37] M. Mazza and D. Zappalà, Phys. Rev. D **64**, 105013 (2001).
[38] A. Bonanno and M. Reuter, J. High Energy Phys. 02 (2005) 035.
[39] D. F. Litim and J. M. Pawlowski, Phys. Rev. D **65**, 081701 (2002).
[40] D. F. Litim and J. M. Pawlowski, Phys. Rev. D **66**, 025030 (2002).
[41] D. F. Litim and J. M. Pawlowski, Phys. Lett. B **546**, 279 (2002).
[42] D. Zappalà, Phys. Rev. D **66**, 105020 (2002).
[43] M. Berzins and P. M. Dew, ACM Trans. Math. Softw. **17**, 178 (1991).
[44] R. Jackiw, Phys. Rev. D **9**, 1686 (1974).
[45] R. Anishetty, R. Basu, N. D. Hari Dass, and H. S. Sharatchandra, Int. J. Mod. Phys. A **14**, 3467 (1999).
[46] J. Engels and T. Mendes, Nucl. Phys. **B572**, 289 (2000).
[47] A. Bonanno and D. Zappalà, Phys. Rev. D **57**, 7383 (1998); A. Bonanno, V. Branchina, H. Mohrbach, and D. Zappalà, Phys. Rev. D **60**, 065009 (1999); G. Andronico, V. Branchina, and D. Zappalà, Phys. Rev. Lett. **88**, 178902 (2002); V. Branchina, H. Faivre, and D. Zappalà, Eur. Phys. J. C **36**, 271 (2004).